Hindawi
Journal of Computer Networks and Communications
Volume 2019, Article ID 4703284, 8 pages
https://doi.org/10.1155/2019/4703284

Research Article

Optimal Packet Length for Free-Space Optical Communications with Average SNR Feedback Channel

Ghassan Alnwaimi[1], **Hatem Boujemaa**[2] **and Kamran Arshad**[3]

[1] *King Abdulaziz University, Jeddah, Saudi Arabia*
[2] *University of Carthage, Sup'Com, COSIM Laboratory, Tunis, Tunisia*
[3] *College of Engineering, Ajman University, Ajman, UAE*

Correspondence should be addressed to Ghassan Alnwaimi; galnwaimi@kau.edu.sa

Received 22 October 2018; Revised 14 April 2019; Accepted 5 May 2019; Published 16 May 2019

Academic Editor: Djamel F. H. Sadok

Copyright © 2019 Ghassan Alnwaimi et al. This is an open access article distributed under the Creative Commons Attribution License, which permits unrestricted use, distribution, and reproduction in any medium, provided the original work is properly cited.

In this article, a method to enhance data rates of free-space optical (FSO) systems using packet length optimization is proposed. The average signal-to-noise ratio (ASNR) is measured at the receiver and sent back to the transmitter to optimize packet length. In addition, the length of packet is optimized to enhance the average throughput. We concluded that packet length can be reduced at low ASNR. However, packet length should be increased at higher values of received ASNR. For each ASNR, we also choose the optimal modulation and coding scheme (MCS) and optimal packet length to maximize the throughput. Different MCSs are investigated such as 4-pulse amplitude modulation (PAM) with and without channel coding, 8-PAM, 16-PAM, and 32-PAM. The proposed method gives 0.8–1.9 dB gain with respect to conventional FSO with adaptive modulation and coding (AMC) and fixed packet length. This is the first paper to deal with packet length optimization for FSO systems.

1. Introduction

FSO communications allow high data rates as compared to radio frequency (RF) communications [1–5]. It is easy to install and does not require uncovering of walkways to introduce fiber joins. Moreover, FSO spectrum is license free. Therefore, FSO communications become viable due to its low implementation cost from one side and to overcome RF spectrum scarcity on the other side. However, the performance of FSO systems can be degraded due to rain, mist, tide, warm, or pointing errors [1–10]. To circumvent this drawback, we can use cooperative or spatial diversity combined with error control coding [11–17]. In cooperative FSO, relays amplify or decode the source message before transmitting it to the destination. Cooperative protocols allow us to benefit from cooperative diversity as the same information is transmitted over independent relayed channels [11–17]. Cooperative communications and channel coding techniques allow us to combat the effects of atmospheric turbulence and improve the performance of FSO systems.

Adaptive modulation and coding (AMC) allows us to increase data rates in free-space optical (FSO) communications. In fact, the best modulation and coding scheme (MCS) is selected for each instantaneous or average SNR. At high SNRs, we can use 32-pulse amplitude modulation (32-PAM) to increase data rates since its spectral efficiency is 5 bit/s/Hz. At low SNR, robust on-off keying (OOK) modulation with channel coding can be used. It is well known that channel coding is required to overcome channel impairments and noise. Different MCSs can be deployed for each range of SNR: i.e., MCS_i is used if $D_i \leq SNR < D_{i+1}$. In this paper, we will provide a methodology to derive the values of thresholds D_i for fixed and optimal packet length. The thresholds for optimal packet length are denoted by D_i, and thresholds for fixed packet length are denoted by S_i.

In all previous studies, packet length is fixed and only the MCS is varied where different-PAM can be used with different channel encoders [18–26]. The main contribution of this paper is to optimize packet length in order to maximize the system throughput. For each average signal-to-noise ratio (ASNR), we choose the optimal packet length and

MCS to have the largest throughput. The proposed solution allows 0.8–1.9 dB gain with respect to conventional FSO systems with AMC and constant packet length. This is the first paper to deal with packet length optimization for FSO systems.

The system model is presented in Section 2. The packet error probability is analyzed in Section 3 in the absence and presence of channel coding. The optimal packet length is derived in Section 4. Adaptive packet length and MCS using ASNR is described in Section 5. Numerical results are given in Section 6. Section 7 concludes the paper.

2. Signal Model

In FSO communications, the received signal is written as follows:

$$y_l = \sqrt{\overline{\Gamma}} g I_p x_l + n_l, \tag{1}$$

where x_l is the transmitted signal, l is the symbol index, g is the atmospheric fading coefficient, I_p is the effect of pointing errors, n_l is an AWGN with normalized variance, and $\overline{\Gamma}$ is the average SNR.

The average SNR can be expressed as follows:

$$\overline{\Gamma} = \frac{E_b}{N_0}, \tag{2}$$

where E_b is the transmitted energy per bit and N_0 is the power spectral density of the noise.

The instantaneous photo SNR is expressed as follows:

$$\gamma = \overline{\Gamma} g^2 I_p^2. \tag{3}$$

We denote

$$h = g^2, \tag{4}$$

as the atmospheric turbulence.

Using a Gamma-Gamma distribution for atmospheric turbulence and in the presence of pointing errors, the probability density function (PDF) is equal to [27]

$$f_\gamma(x) = \frac{b^2}{x\Gamma(\zeta)\Gamma(\varepsilon)} G_{1,3}^{3,0}\left[\zeta\varepsilon\frac{x}{\overline{\Gamma}}\bigg|_{b^2,\zeta,\varepsilon}^{b^2+1}\right], \tag{5}$$

where G is Meijer's G function and b is the ratio between the equivalent beam radius at the receiver and pointing error displacement standard deviation. For small pointing errors, i.e., $b \longrightarrow +\infty$, the above distribution converges to the nonpointing error case, where $\zeta = 2.064$ and $\varepsilon = 1.342$ correspond to strong turbulence, $\zeta = 2.296$ and $\varepsilon = 1.822$ correspond to moderate turbulence, and $\zeta = 2.902$ and $\varepsilon = 2.51$ correspond to weak turbulence [28, 29].

The cumulative distribution (CDF) of SNR is given by the following equation [27]:

$$F_\gamma(x) = \frac{b^2}{x\Gamma(\zeta)\Gamma(\varepsilon)} G_{2,4}^{3,1}\left[\zeta\varepsilon\frac{x}{\overline{\Gamma}}\bigg|_{b^2,\zeta,\varepsilon}^{1,b^2+1}\right]. \tag{6}$$

3. Preliminary Results

The average packet error probability (PEP) can be tightly upper bounded by the following equation [30]:

$$\text{PEP} \le \int_0^{w_0} f_\gamma(x)dx = F_\gamma(w_0), \tag{7}$$

where $f_\Gamma(\gamma)$ is the PDF of SNR Γ and w_0 is a waterfall threshold.

Equation (7) shows that the PEP for a given instantaneous SNR $\gamma \le w_0$ is approximated by 1. However, the PEP for a given instantaneous SNR $\gamma > w_0$ is approximated by 0.

The waterfall threshold can be written as follows [30]:

$$w_0 = \int_0^{+\infty} g(\gamma)d\gamma, \tag{8}$$

where $g(\gamma)$ is the PEP for a given instantaneous SNR γ.

3.1. Without Channel Coding

3.1. Without Channel Coding. For uncoded M-PAM, we have

$$g(\gamma) = 1 - (1 - P_{es}(\gamma))^{((N+n_d)/(\log_2(M)))}, \tag{9}$$

where N is the number of data bits per packet, n_d is the number of parity bits per packet, and P_{es} is the symbol error probability (SEP) of M-PAM [31].

$$P_{es}(\gamma) = \frac{M-1}{M}\operatorname{erfc}\left(\sqrt{\frac{3\gamma\log_2(M)}{2(M-1)(2M-1)}}\right), \tag{10}$$

using

$$\operatorname{erfc}(x) \le e^{-x^2}. \tag{11}$$

Using (10) and (11), we have

$$P_{es} \simeq a_1 e^{-c_1\gamma}, \tag{12}$$

where

$$a_1 = \frac{M-1}{M}, \qquad c_1 = \frac{3\log_2(M)}{2(M-1)(2M-1)}. \tag{13}$$

3.2. With Channel Coding. For convolutionally coded communications, we have

$$g(\gamma) = 1 - (1 - P_E(\gamma))^{((N+n_d)/\log_2(M))}, \tag{14}$$

where

$$P_E(\gamma) \le \sum_{d=d_f}^{+\infty} a_d P_d(\gamma), \tag{15}$$

in which d_f and a_d are, respectively, the free distance and distance spectrum.

$$P_d(\gamma) \simeq \frac{M-1}{M} \operatorname{erfc}\left(\sqrt{\frac{R_c d 3\gamma \log_2(M)}{2(M-1)(2M-1)}}\right), \quad (16)$$

where R_c is the rate of convolutional encoding.

Using equation (11), we have

$$P_E(\gamma) \simeq a_2 e^{-c_2\gamma}, \quad (17)$$

where

$$a_2 = a_{d_f}\frac{M-1}{M}, \qquad c_2 = \frac{R_c d_f 3\log_2(M)}{2(M-1)(2M-1)}. \quad (18)$$

We have

$$g(\gamma) \simeq 1-\left(1-a_i e^{-c_i\gamma}\right)^{((N+n_d)/(\log_2(M)))}, \quad (19)$$

where $i = 1$ for coded communications and $i = 2$ for uncoded communications.

3.3. Waterfall Threshold. Appendix shows that waterfall threshold is written as

$$w_0 \simeq k_1 \ln\left(\frac{N+n_d}{\log_2(M)}\right) + k_2, \quad (20)$$

where

$$k_1 = \frac{1}{c_i}, \qquad k_2 = \frac{E+\ln(a_i)}{c_i}, \quad (21)$$

where $E \simeq 0.577$ is the Euler constant.

4. Optimal Packet Length Using ASNR

The number of trials of HARQ is [32–34] calculated as follows:

$$T_r = \sum_{i=1}^{+\infty} i\,\mathrm{PEP}^{i-1}(1-\mathrm{PEP}) = \frac{1}{1-\mathrm{PEP}}. \quad (22)$$

The throughput in bit/s/Hz is expressed as follows:

$$\mathrm{Thr} = \frac{\log_2(M)N}{(N+n_d)T_s B T_r} = \frac{\log_2(M)N}{(N+n_d)}(1-\mathrm{PEP}) > \frac{\log_2(M)N}{(N+n_d)}\left[1-F_\gamma(w_0)\right], \quad (23)$$

where $B = 1/T_s$ is the used bandwidth and T_s is the symbol period. In equation (23), we used the expression of PEP provided in equation (7).

The optimal packet length maximizing the throughput can be obtained using the gradient algorithm:

$$N_{i+1} = N_i + \mu\frac{\partial \mathrm{Thr}(N=N_i)}{\partial N}. \quad (24)$$

Usually, the gradient search is used to minimize a function f, and we write $N_{i+1} = N_i - \mu((\partial f(N=N_i))/\partial N)$. Here, we aim to maximize the throughput which is equivalent to minimize $f = -\mathrm{Thr}$.

The derivative of throughput with respect to packet length is equal to

$$\frac{\partial \mathrm{Thr}}{\partial N} = \frac{\log_2(M)nd}{(N+n_d)^2}\left[1-F_\gamma(w_0)\right] - \frac{\log_2(M)N}{(N+n_d)} f_\gamma(w_0) \times \frac{k_1}{N+n_d}. \quad (25)$$

This expression is valid for Gamma-Gamma atmospheric turbulence with pointing errors.

The used packet length is the closed solution to that obtained by gradient search such that $N+n_d$ is a multiple of $\log_2(M)$ so that bits can be converted to $(N+n_d)/\log_2(M)$ M-PAM symbols.

5. Optimal Packet Length with AMC

Figure 1 shows the average throughput of FSO communications with respect to ASNR using optimal N obtained with gradient search equation (24). From Figure 1, we can deduce the following strategy:

(i) $\overline{\Gamma} < D_1 = 14.5$ dB: use convolutionally coded 4-PAM $R_c = 1/2$
(ii) $D_1 < \overline{\Gamma} < D_2 = 22.2$ dB: use uncoded 4-PAM
(iii) $D_2 < \overline{\Gamma} < D_3 = 29.2$ dB: use uncoded 8-PAM
(iv) $D_3 < \overline{\Gamma} < D_4 = 35.9$: use uncoded 16-PAM
(v) $D_4 < \overline{\Gamma}$: use uncoded 32-PAM

Thresholds D_i correspond to intersection of different curves in Figure 1.

As shown in Figure 2, a similar approach is used when packet length is fixed, $N = 410$ and $n_d = 10$ with thresholds $S_1 = 16.1$ dB, $S_2 = 23.3$ dB, and $S_3 = 30$ dB.

Figure 3 shows the proposed adaptive packet length and adaptive MCS using ASNR $\overline{\Gamma}$. The ASNR is measured at the receiver to select the optimal packet length and MCS. The ASNR is compared to thresholds D_1, D_2, D_3, and D_4 to determine the optimal MCS. Packet length is computed using the gradient algorithm as explained in equations (24) and (25) .

6. Numerical Results

Numerical results were obtained in the presence of both atmospheric turbulence and pointing errors. Except in Figure 4, the ratio b between the equivalent beam radius at receiver and pointing error displacement standard deviation is 12. Weak, moderate, and strong turbulence were considered. Figures 5 and 6 show, respectively, the average throughput of FSO communications for 4-PAM, ASNR = 15 dB (respectively, ASNR = 20 dB) with respect to packet length N. In all results, $n_d = 10$. We notice that throughput can be maximized by optimizing packet length.

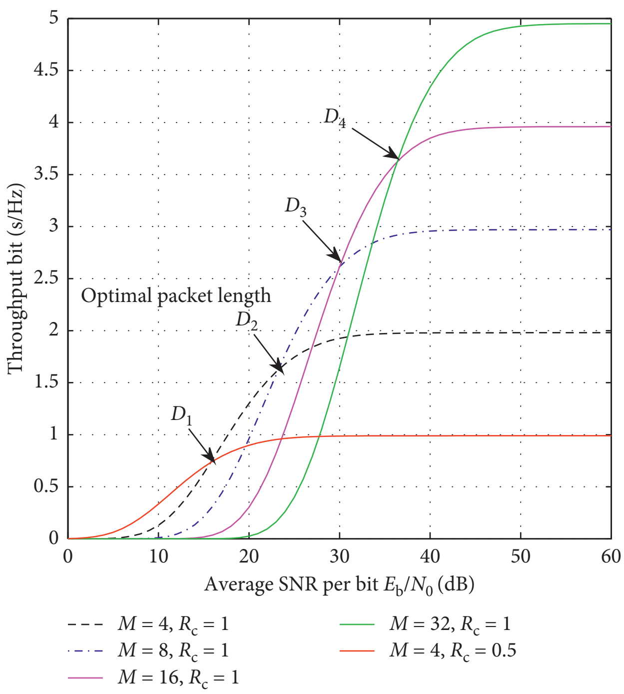

FIGURE 1: Average throughput of FSO systems for optimal packet length and different modulations and coding schemes with moderate turbulence.

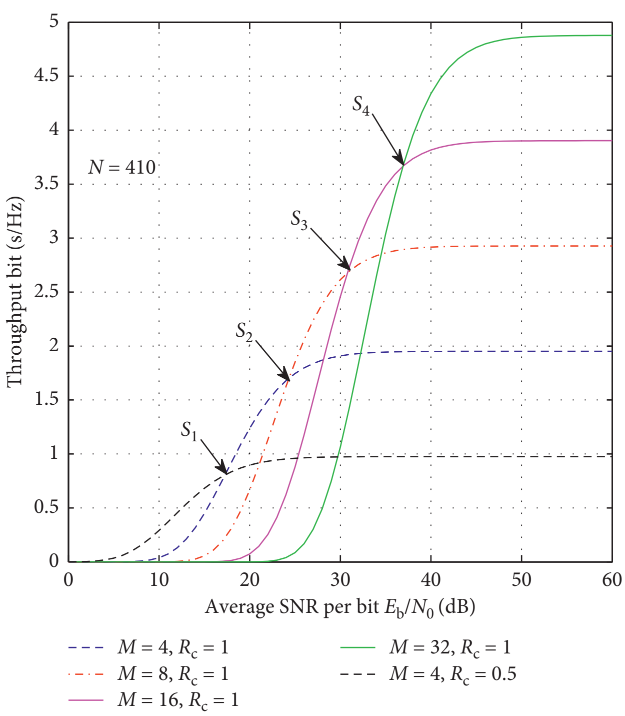

FIGURE 2: Average throughput of FSO systems for fixed packet length and different modulations and coding schemes with moderate turbulence.

In fact, we notice that we can choose the value of packet length N to maximize the throughput. As shown in Figure 5, increasing packet length does not mean increasing the throughput all the time and there is a certain length that maximizes the throughput. The optimal packet length increases as the average SNR increases, as shown in Figures 5 and 6. The optimal packet length is 60 (respectively, 120) for $E_b/N_0 = 15$ dB (respectively, 20 dB). By comparing the results of Figures 5 and 6, we concluded that packet length should be increased as the ASNR increases.

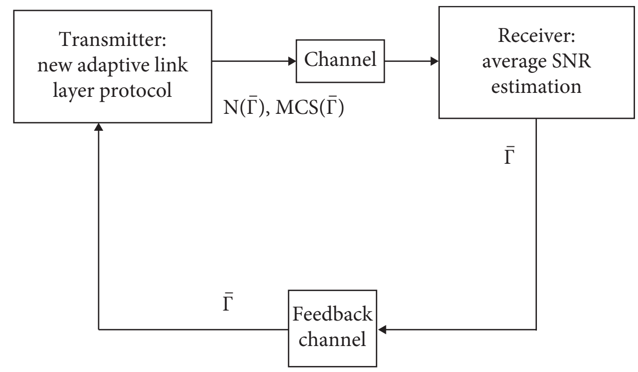

FIGURE 3: Packet length optimization using ASNR.

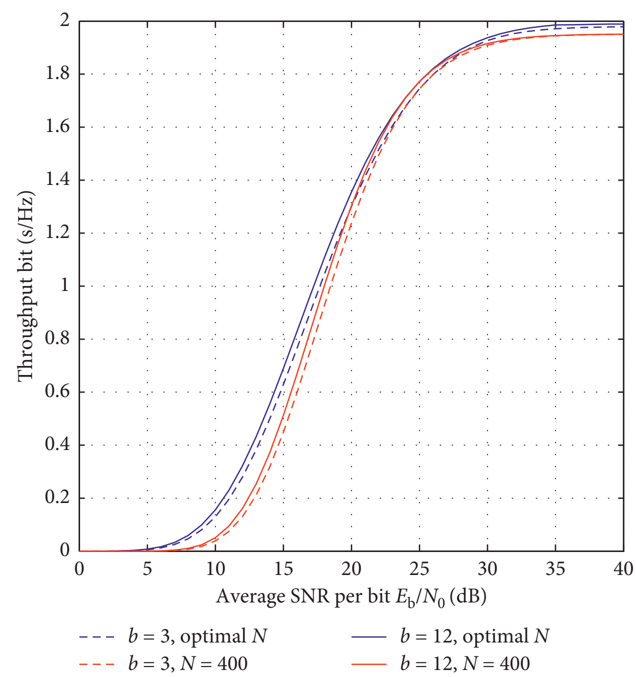

FIGURE 4: Effect of pointing errors.

Figure 7 compares the average throughput of 4-PAM when packet length is optimal with respect to the fixed packet length (FPL) N of 200, 400, and 1000. We notice that packet length optimization allows 0.8 dB gains with respect to $N = 200$ and throughput equal to 0.5 bit/s/Hz. Optimal packet length allows 1.3 dB gains with respect to $N = 400$ and throughput equal to 0.5 bit/s/Hz. Optimal packet length allows 1.9 dB gains with respect to $N = 1000$ and throughput equal to 0.5 bit/s/Hz. At high ASNR, $N = 1000$ allows higher throughput than $N = 400$ and $N = 200$. At low ASNR, $N = 200$ allows higher throughput than $N = 400$ and $N = 1000$.

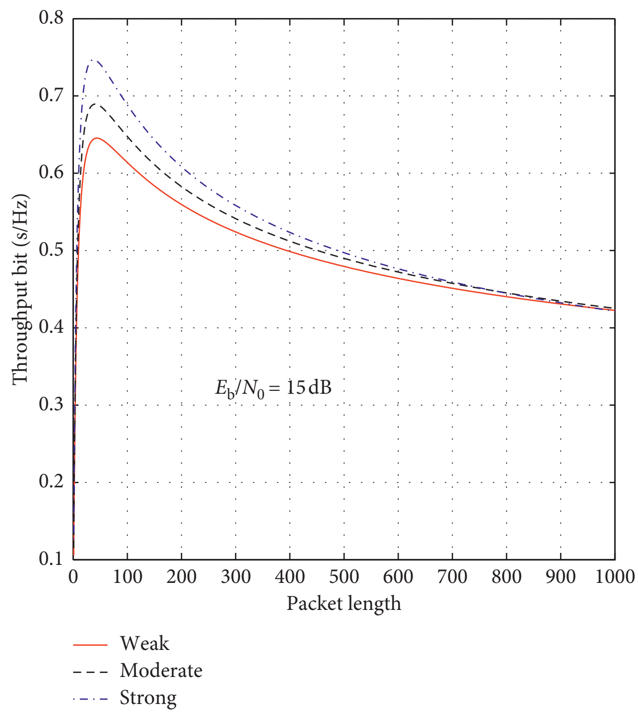

Figure 5: Average throughput of FSO systems with respect to packet length for an average SNR of 15 dB.

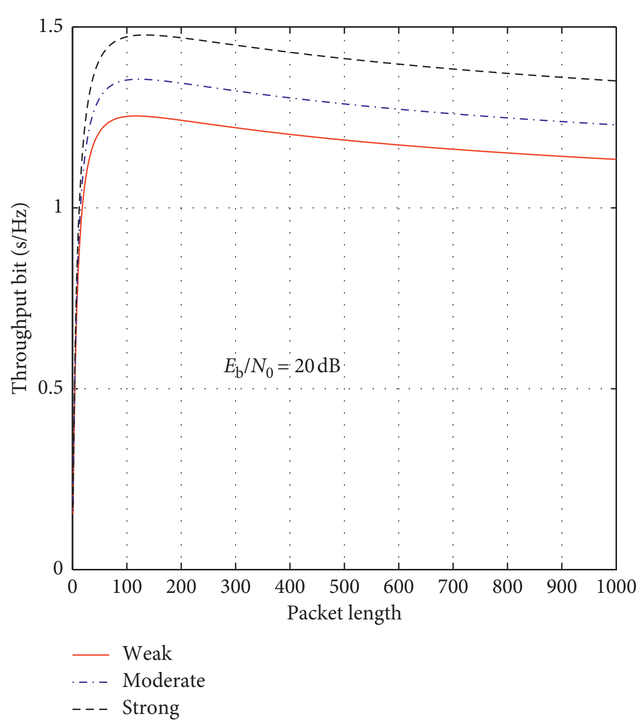

Figure 6: Average throughput of FSO systems with respect to packet length for an average SNR of 20 dB.

Figure 1 shows the average throughput of FSO communications with optimal packet length for different modulations and coding schemes (MCSs): 4-PAM with R_c = 0.5 convolutional coding; 4-PAM, 8-PAM, 16-PAM, and 32-PAM without channel coding. The following AMC strategy is suggested:

(i) $\overline{\Gamma} < D_1 = 14.5$ dB: use convolutionally coded 4-PAM with $R_c = 1/2$

(ii) $D_1 < \overline{\Gamma} < D_2 = 22.2$ dB: use uncoded 4-PAM

(iii) $D_2 < \overline{\Gamma} < D_3 = 29.2$ dB: use uncoded 8-PAM

(iv) $D_3 < \overline{\Gamma} < D_4 = 35.9$ dB: use uncoded 16-PAM

(v) $D_4 < \overline{\Gamma}$: use uncoded 32-PAM

The thresholds D_i correspond to the intersection of different curves.

Figure 2 shows the average throughput of FSO communications with $N = 410$ for different modulations and coding schemes (MCSs): 4-PAM with $R_c = 0.5$ convolutional coding; 4-PAM, 8-PAM, 16-PAM, and 32-PAM without channel coding. If 4-PAM is used, the packet of length $N + n_d = 420$ is converted to $420/2 = 210$ symbols. If 8-PAM is used, the packet is converted to $420/3 = 140$ symbols. If 16-PAM is used, the packet is converted to $420/4 = 105$ symbols. If 32-PAM is used, the packet is converted to $420/5 = 84$ symbols. Therefore, packet length should be a multiple of 60.

The following AMC approach is suggested:

(i) $\overline{\Gamma} < S_1 = 16.1$ dB: use 4-PAM with convolutional coding $R_c = 1/2$

(ii) $S_1 < \overline{\Gamma} < S_2 = 23.3$ dB: use uncoded 4-PAM

(iii) $S_2 < \overline{\Gamma} < S_3 = 30$ dB: use uncoded 8-PAM

(iv) $S_3 < \overline{\Gamma} < S_4 = 36.4$ dB: use uncoded 16-PAM

(v) $S_4 < \overline{\Gamma}$: use uncoded 32-PAM. Packet length is equal to $N = 410$

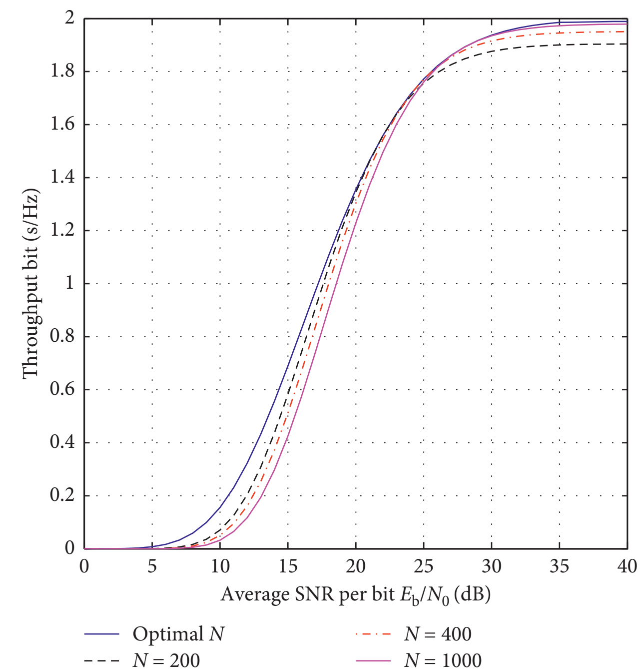

Figure 7: Average throughput of FSO systems for optimal and fixed packet length: 4-PAM modulation and moderate turbulence.

Thresholds S_i correspond to intersection of different curves.

4-PAM transmits 2 bits per symbol, whereas 5 bits are coded in one 32-PAM symbol. As the number of bits per symbol increases, the spectral efficiency increases, but the PEP also increases since the symbols are closer to each other for a fixed transmit energy per bit.

Figure 8 shows the throughput of FSO systems with adaptive modulation and coding (AMC) for fixed and adaptive packet length. Optimal packet length offers 1 dB gain with respect to $N = 410$. The curve of optimal packet length with AMC is the upper bound of 5 curves of Figure 1. The curve of fixed packet length $N = 410$ with AMC is the upper bound of 5 curves of Figure 2.

The effects of pointing errors are investigated in Figure 4 for $b = 3$ and $b = 12$. b is the ratio between the equivalent beam radius at the receiver and pointing error displacement standard deviation. We notice that the proposed optimal packet length allows us to increase the throughput even in the presence of pointing errors. When b is small, the pointing errors increase and the throughput decreases.

We compare in Figure 9 the throughput derived in our paper for $N=400$ to that obtained from [27]. We used the PDF of SNR [27] to compute the PEP and throughput of 4-PAM as an integral as follows:

$$\mathrm{PEP} = \int_0^{+\infty} g(x) f_\Gamma(x) dx, \tag{26}$$

where $g(x)$ is the PEP for SNR equal to x, as given in equation (12).

Another contribution of the paper is to show that PEP can be deduced from CDF of SNR and yields close results to the PEP computed using the above integral. Figure 9 shows that our results are very close to those of [27]. We have provided in equation (10) a tight upper bound of PEP. Therefore, it is a tight lower bound on throughput.

7. Conclusion

In this paper, we have optimized the throughput for FSO communications. For each average SNR (ASNR), we choose the optimal packet length and MCS to have the largest throughput. Optimal packet length was obtained using the gradient search algorithm and yields 0.8–1.9 dB gain with respect to conventional FSO. We have shown that the optimal packet length should be increased with average SNR to obtain higher throughput. We have also identified threshold to select the appropriate MCS for each average SNR and ensure higher data rates. The average SNR is compared to thresholds: when average SNR (ASNR) is less than 14.5 dB, 4-PAM with half-rate channel coding is used. When 14.5 dB < ASNR ≤ 22.2 dB, uncoded 4-PAM is the best choice. When 22.2 dB < ASNR ≤ 29.2 dB, uncoded 8-PAM should be used. When 29.2 dB < ASNR ≤ 35.9 dB, uncoded 16-PAM is the best choice. When 35.9 dB < ASNR, uncoded 32-PAM is the best choice. In all ranges of SNR, an optimal packet length has been used with each optimal MCS.

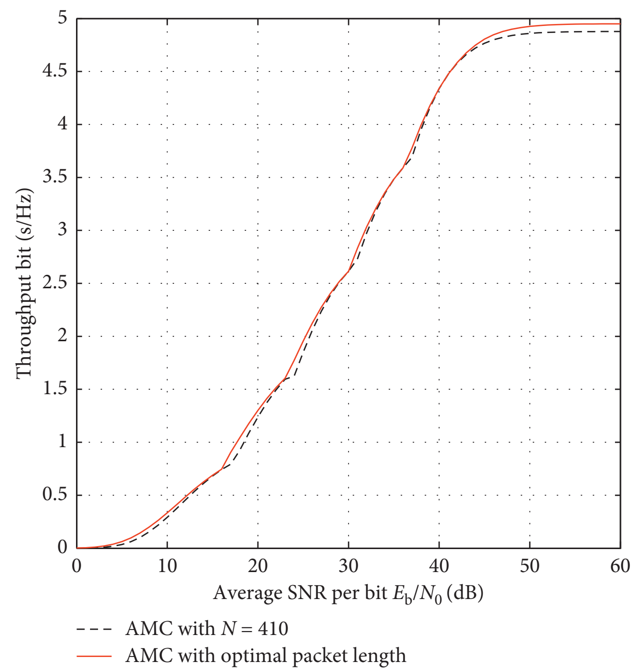

FIGURE 8: Throughput of FSO systems with AMC using ASNR: fixed versus optimal packet length and moderate turbulence.

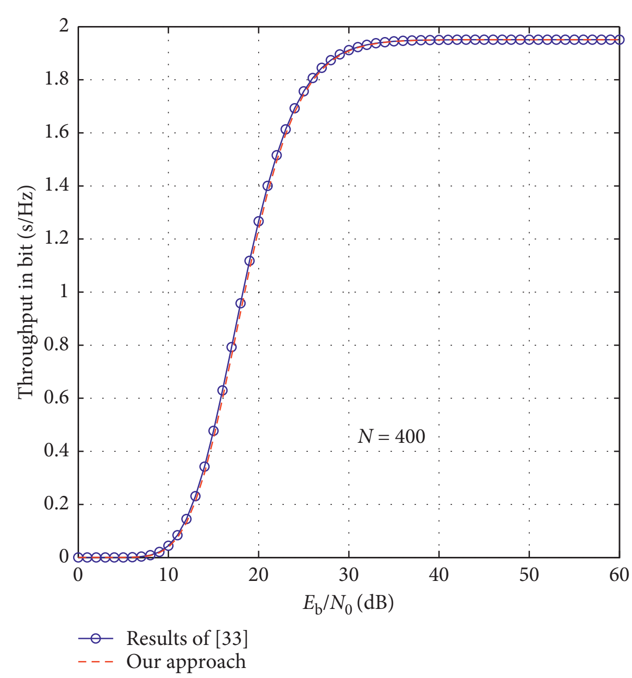

FIGURE 9: Throughput computation using an integral and our approach.

Appendix

We have

$$w_0 = \int_0^{+\infty} \left[1 - \left(1 - a_i e^{-c_i u}\right)^{((N+n_d)/\log_2(M))}\right] du. \tag{A.1}$$

Let $y = a_i e^{-c_i u}$, and we deduce

$$w_0 = \frac{1}{c_i}\int_0^{a_i}\left[1-(1-y)^{\left((N+n_{\mathrm{d}})/\log_2(M)\right)}\right]\frac{dy}{y}. \tag{A.2}$$

We deduce

$$w_0 = \frac{1}{c_i}\int_{1-a_i}^{1}\frac{1}{1-x}\left[1-x^{\left((N+n_{\mathrm{d}})/\log_2(M)\right)}\right]dx. \tag{A.3}$$

We deduce

$$w_0 = \frac{1}{c_i}\int_{1-a_i}^{1}\sum_{k=0}^{\left((N+n_{\mathrm{d}})/\log_2(M)\right)-1}x^k dx. \tag{A.4}$$

We deduce

$$w_0 = \frac{1}{c_i}\sum_{k=1}^{(N+n_{\mathrm{d}})/\log_2(M)}\left(\frac{1}{k}-\frac{(1-a_i)^k}{k}\right). \tag{A.5}$$

For $((N+n_{\mathrm{d}})/\log_2(M)) \gg 1$, we can write

$$\sum_{k=1}^{(N+n_{\mathrm{d}})/\log_2(M)}\frac{1}{k} = \ln\left(\frac{N+n_{\mathrm{d}}}{\log_2(M)}\right)+E, \tag{A.6}$$

$$\sum_{k=1}^{(N+n_{\mathrm{d}})/\log_2(M)}\frac{(1-a_i)^k}{k} \simeq \sum_{k=1}^{+\infty}\frac{(1-a_i)^k}{k} = -\ln(a_i). \tag{A.7}$$

Combining equations (A.5)–(A.7), we obtain (20).

Data Availability

No data were used to support this study.

Conflicts of Interest

The authors declare that they have no conflicts of interest.

References

[1] I. B. Djordjevic, "Adaptive modualtion and coding for free space optical channel," *Journal of Optical Communications and Networking*, vol. 2, no. 5, p. 221, 2010.

[2] E. Zedini, A. Chelly, and M. S. Alouini, "On the performance analysis of hybrid ARQ with incremental redundancy and with code combining over free space optical channels with pointing errors"," *IEEE Photonics Journal*, vol. 6, no. 4, pp. 1–18, 2014.

[3] E. Zedini, A. Chelly, and M. S. Alouini, "Unified performance analysis of hybrid arq with incremental redundancy over free space optical channels," in *Proceedings of the 2014 IEEE 25th Annual International Symposium on Personal, Indoor, and Mobile Radio Communication (PIMRC2014)*, Bologna, Italy, September 2014.

[4] S. Aghajanzadeh and M. Uysal, "Outage analysis of hybrid arq protocols in coherent free space optical communications," in *Proceedings of the 2011 IEEE 22nd International Symposium on Personal, Indoor and Mobile Radio Communications (PIMRC)*, Toronto, Canada, 2011.

[5] S. Aghajanzadeh and M. Uysal, "Information theoretic analysis of hybrid ARQ protocols in coherent free space optical communications," *IEEE Transactions on Communications*, vol. 60, no. 5, pp. 1432–1442, 2012.

[6] M. R. Bhatnagar and M. K. Arti, "Performance analysis of hybrid satellite-terrestrial FSO cooperative system," *IEEE Photonics Technology Letters*, vol. 25, no. 22, pp. 2197–2200, 2013.

[7] N. A. Mohd Nor, Z. Ghassemlooy, J. Bohata et al., "Experimental investigation of all-optical relay-assisted 10 Gb/s FSO link over the atmospheric turbulence channel," *Journal of Lightwave Technology*, vol. 35, no. 1, pp. 45–53, 2017.

[8] A. Jaiswal, M. R. Bhatnagar, and V. K. Jain, "Performance evaluation of space shift keying in free-space optical communication," *Journal of Optical Communications and Networking*, vol. 9, no. 2, pp. 149–160, 2017.

[9] A. A. Farid and S. Hranilovic, "Outage capacity optimization for free-space optical links with pointing errors," *Journal of Lightwave Technology*, vol. 25, no. 7, pp. 1702–1710, 2007.

[10] M. R. Bhatnagar and Z. Ghassemlooy, "Performance analysis of gamma-gamma fading FSO MIMO links with pointing errors," *Journal of Lightwave Technology*, vol. 34, no. 9, pp. 2158–2169, 2016.

[11] E. Zedini and M.-S. Alouini, "Multihop communications over CSI-assisted relay IM/DD FSO systems with pointing errors," in *Proceedings of the IEEE International Conference on Communication Workshop (ICCW)*, pp. 937–942, 2015.

[12] L. Yang, X. Gao, and M.-S. Alouini, "Performance analysis of relay-assisted all-optical FSO networks over strong atmospheric turbulence channels with pointing errors"," *Journal of Lightwave Technology*, vol. 32, no. 23, pp. 4613–4620, 2014.

[13] M. R. Bhatnagar, "Average BER analysis of relay selection based decode-and-forward cooperative communication over gamma-gamma fading FSO links," in *Proceedings of the IEEE International Conference on Communications (ICC)*, pp. 3142–3147, Budapest, Hungary, 2013.

[14] S. Anees and M. R. Bhatnagar, "Performance of an amplify-and-forward dual-hop asymmetric RF-FSO communication system," *Journal of Optical Communications and Networking*, vol. 7, no. 2, pp. 124–135, 2015.

[15] I. S. Ansari, F. Yilmaz, and M.-S. Alouini, "Impact of pointing errors on the performance of mixed RF/FSO dual-hop transmission systems," *IEEE Wireless Communications Letters Year*, vol. 2, no. 3, pp. 351–354, 2013.

[16] E. Lee, J. Park, D. Han, and G. Yoon, "Performance analysis of the asymmetric dual-hop relay transmission with mixed RF/FSO links," *IEEE Photonics Technology Letters*, vol. 23, no. 21, pp. 1642–1644, 2011.

[17] B. He and R. Schober, "Bit-interleaved coded modulation for hybrid RF/FSO systems," *IEEE Transactions on Communications*, vol. 57, no. 12, pp. 3753–3763, 2009.

[18] V. V. Mai, T. C. Thang, and A. T. Pham, "Performance analysis of TCP over free space optical links with ARQ-SR," in *Proceedings of the 18-th European Conference on Network and Optical Communications*, Graz, Austria, July 2013.

[19] G. Prakash and M. Kulkarmi, "On the performance of luby transform codes over selective repeat ARQ in turbulent free space optical links," in *Proceedings of the IEEE International Conference on Computational Science and Engineering*, Sydney, Australia, 2013.

[20] K. Fatima, S. Sheikh Muhammad, and E. Leitgeb, "Adaptive coded modulation for FSO links," in *Proceedings of the 8th International Symposium on Communication Systems, Networks Digital Signal Processing (CSNDSP)*, pp. 1–4, Poznan, Poland, July 2012.

[21] A. Jaiswal, V. K. Jain, and S. Kar, "Adaptive coding and modulation (ACM) technique for performance enhancement of FSO Link," in *Proceedings of the IEEE First International*

Conference on Control, Measurement and Instrumentation (CMI), pp. 53–57, Kolkata, India, 2016.

[22] G.-H. Gho and J. M. Kahn, "Rate-adaptive modulation and low-density parity-check coding for optical fiber transmission systems"," *IEEE/OSA Journal of Optical Communications and Networking*, vol. 4, no. 10, pp. 760–768, 2012.

[23] G.-H. Gho and J. M. Kahn, "Rate-adaptive modulation and coding for optical fiber transmission systems," *Journal of Lightwave Technology*, vol. 30, no. 12, pp. 1818–1828, 2012.

[24] J. L. Gao, "A study of adaptive coding and modulation over free space optical link using OCTL data," in *Proceedings of the 2016 IEEE Aerospace Conference*, pp. 1–7, Big Sky, MT, USA, 2016.

[25] Y. Zeng, R. J. Green, and M. S. Leeson, "Adaptive pulse amplitude and position modulation for optical wireless channels," in *Proceedings of the 2nd IET International Conference on Access Technologies*, pp. 13–16, Cambridge, UK, June 2006.

[26] S. Hasan Hariq, N. Odabasioglu, and M. Uysal, "An adaptive modulation scheme for coded free-space optical systems," in *Proceedings of the 19th European Conference on Networks and Optical Communications—(NOC)*, pp. 132–135, Milan, Italy, June 2014.

[27] I. S. Ansari, F. Yilmaz, and M.-S. Alouini, "On the performance of mixed RF/FSO variable gain dual-hop transmission systems with pointing errors," in *Proceedings of the IEEE 78th Vehicular Technology Conference (VTC Fall)*, Las Vegas, NV, USA, 2013.

[28] H. G. Sandalidis, T. A. Tsiftsis, G. K. Karagiannidis, and M. Uysal, "BER performance of FSO links over strong atmospheric turbulence channels with pointing errors," *IEEE Communications Letters*, vol. 12, no. 1, pp. 44–46, 2008.

[29] J. Park, E. Lee, and G. Yoon, "Average bit-error rate of the Alamouti scheme in gamma-gamma fading channels," *IEEE Photonics Technology Letters*, vol. 23, no. 4, pp. 269–271, 2011.

[30] Y. Xi, A. Burr, J. Wei, and D. Grace, "A general upper bound to evaluate packet error rate over quasi-static fading channels," *IEEE Transactions on Wireless Communications*, vol. 10, no. 5, pp. 1373–1377, 2011.

[31] J. G. Proakis, *Digital Communications*, McGraw-Hill, New York, NY, USA, 3rd edition, 1995.

[32] H. Boujemaa, "Delay analysis of cooperative truncated HARQ with opportunistic relaying," *IEEE Transactions on Vehicular Technology*, vol. 58, no. 9, pp. 4795–4804, 2009.

[33] J. A. Anguita, I. B. Djordjevic, M. A. Neifeld, and B. V. Vasic, "Shannon capacities and error-correction codes for optical atmospheric turbulent channels," *Journal of Optical Networking*, vol. 4, no. 9, pp. 586–601, 2005.

[34] S. Al-Ahmadi and H. Yanikomeroglu, "On the approximation of the generalized-K distribution by a gamma distribution for modeling composite fading channels," *IEEE Transactions on Wireless Communications*, vol. 9, no. 2, pp. 706–713, 2010.


Journal of Engineering
The Scientific World Journal
International Journal of Rotating Machinery
Journal of Sensors
Advances in Multimedia
Advances in Civil Engineering
Hindawi
Submit your manuscripts at
www.hindawi.com
Journal of Control Science and Engineering
Journal of Robotics
Journal of Electrical and Computer Engineering
Advances in OptoElectronics
VLSI Design
International Journal of Navigation and Observation
Modelling & Simulation in Engineering
International Journal of Aerospace Engineering
International Journal of Chemical Engineering
International Journal of Antennas and Propagation
Active and Passive Electronic Components
Shock and Vibration
Advances in Acoustics and Vibration